



## Antenna as sensors: a mini review

Rafsan Al Shafatul Islam Subad, Mennatallah F. El Kashouty and Siddhartha Das \*Cite this: *J. Mater. Chem. C*, 2025, 13, 20862Received 14th July 2025,  
Accepted 23rd September 2025

DOI: 10.1039/d5tc02661j

rsc.li/materials-c

Antenna-based sensors are emerging as a transformative class of multifunctional devices that unify wireless communication and environmental sensing within a single, compact architecture. Unlike conventional systems that rely on separate sensing and transmission units, antenna sensors leverage the intrinsic electromagnetic sensitivity of antenna structures to detect physical, chemical, or biological parameters such as temperature, humidity, strain, and pH. By embedding or coating antennas with responsive materials or designing them to react to changes in the surrounding dielectric environment, these systems can modulate key properties—such as resonance frequency, return loss, or radiation pattern—in response to external stimuli. This dual-functionality enables real-time, wireless monitoring with significantly reduced component count, enhanced power efficiency, and, in many cases, fully passive operation. Furthermore, recent advances in flexible materials, additive manufacturing, and miniaturized design have expanded the versatility of antenna sensors for applications in wearable electronics, structural health monitoring, biomedical diagnostics, and the Internet of Things (IoT). This article presents a mini review on the principles, architectures, and opportunities of antenna-based sensors, emphasizing their potential to redefine the paradigm of distributed, low-power sensing systems.

## 1 Introduction

For more than a century, antennas have been at the heart of wireless communications. In recent years, however, antennas have emerged not only as passive components for wireless communication but also as active elements capable of acting as highly efficient sensors.<sup>1–6</sup> This dual functionality has garnered increasing attention, particularly within the fields of structural health monitoring,<sup>7</sup> biomedical diagnostics,<sup>4</sup> chemical sensing,<sup>8</sup> and wearable electronics.<sup>3</sup> The ability of antennas to detect variations in different physical, chemical, or biological quantities with high efficiency stems from their intrinsic sensitivity to changes in dielectric properties, geometry, or nearby materials, which directly influence their electromagnetic responses such as resonance frequency, impedance, or radiation pattern.<sup>9,10</sup>

Unlike conventional sensors that often require discrete transducers and power-intensive signal conditioning, antenna-based sensors offer a unique combination of simplicity, wireless operability, and high spatial and temporal resolution. Their ability to operate in passive, battery-less modes makes them especially appealing for remote or embedded applications,<sup>3,11</sup> where conventional (wired) sensors are impractical/infeasible or where power delivery is limited [*e.g.*,

in remote infrastructure monitoring, implantable biomedical devices, or distributed internet of things (IoT) networks<sup>12,13</sup>]. Additionally, antenna sensors inherently support real-time and non-invasive measurements, making them suitable for applications ranging from environmental monitoring and food safety to structural health diagnostics and wearable health technologies.<sup>14,15</sup>

With the advent of advanced fabrication techniques (*e.g.*, different types of 3D printing) and the discovery of novel materials (*e.g.*, metamaterials, nanomaterials, and conductive polymers), the design space for antenna sensors has significantly expanded, enabling multifunctional, miniaturized, and conformable sensing platforms.<sup>10</sup> For example, recent advancements in 3D printing enabling fabrication of electronic devices on flexible and highly curved substrates, it has become possible to develop conformal and stretchable antenna sensors that can seamlessly integrate with various substrates and surfaces, including textiles, composites, and biological tissues.<sup>16–20</sup> Similarly, the discovery of novel materials (*e.g.*, metamaterials, 2D and 1D nanomaterials, *etc.*) and their integration into reconfigurable electronics have led to the fabrication of antenna structures with enhanced sensitivity, tunability, and multifunctionality, pushing the boundaries of what can be achieved in smart sensing platforms.<sup>21–23</sup>

Building on this foundation, antenna-based sensors are gaining increasing popularity as a strategic technological convergence of electromagnetic design, materials engineering, and embedded sensing. Their ability to integrate seamlessly into

Department of Mechanical Engineering, University of Maryland College Park, Glenn L. Martin Hall, 4298 Campus Dr, College Park, MD 20742, USA.  
E-mail: [sidd@umd.edu](mailto:sidd@umd.edu)



wireless systems enables a reduction in hardware redundancy, particularly by eliminating the need for separate transducers and communication modules in applications such as implantable biomedical devices and wearable systems.<sup>24–26</sup> Beyond traditional geometries, recent developments in fractal, conformal, and metamaterial-inspired antenna structures have introduced even greater adaptability in tailoring frequency responses and enhancing spatial sensitivity to external perturbations.<sup>9,27–29</sup> These structural variations allow antennas to be finely tuned to detect diverse parameters—including chemical vapors, humidity, mechanical strain, and thermal gradients—with both passive and active configurations depending on the sensing environment.<sup>19,30–33</sup> As the demands of modern applications increasingly require scalable, low-power, and distributed sensing capabilities, antenna sensors provide a promising foundation for next-generation systems such as the Internet of Things (IoT), environmental monitoring networks, and autonomous structural diagnostics.<sup>14,34</sup> Rather than serving as auxiliary components, antennas in these contexts become multifunctional platforms, capable of simultaneously enabling communication and contextual awareness within a compact, energy-efficient form factor. Despite these advances, challenges remain in terms of sensitivity, selectivity, environmental robustness, and standardization of sensing protocols. Furthermore, the complexity of accurately modeling the multiphysical interactions between antenna structures and dynamic sensing environments requires continued development of computational tools and experimental validation methods. Nevertheless, the growing convergence of antenna engineering, materials science, and sensor technology heralds a future where antennas are no longer just communication components, but intelligent nodes capable of perceiving and responding to their surroundings.

This mini review (1) explores the evolution of antennas into sensing devices, (2) examines the underlying physical principles that enable this functionality, and (3) seeks to outline the current landscape and future directions of antenna-based sensing (or the development of next-generation antenna-based sensors that leverage the recent advances in 3D printing and artificial intelligence), emphasizing the multidisciplinary opportunities and challenges ahead. By framing antennas as both emitters and sensors, we move toward a future of more compact, efficient, and integrated systems that redefine the boundaries of wireless sensing and communication.

## 2 Brief history and mechanism of antenna based sensing

Antenna was first developed by Heinrich Rudolph Hertz in 1888.<sup>35,36</sup> The initial sensing activities by antennas included electric and magnetic field sensing to detect mines, metals, and weapons during wars. Later on, the scope of sensing by antennas expanded into archaeological exploration and infrastructure analysis. Radar-based sensing, which relies on antennas to transmit and receive electromagnetic waves, enables

object detection, localization, and velocity measurement. Ground-penetrating radars, for instance, utilize antennas to detect buried structures and objects. In antenna-based sensing, the core mechanism relies on the antenna's sensitivity to changes in its surrounding electromagnetic environment. When exposed to physical, chemical, or biological stimuli, such as strain, temperature, humidity, or variations in tissue composition, these external factors can alter the antenna's effective permittivity, conductivity, or geometry.<sup>3,9,10</sup> Such changes influence the antenna's key electromagnetic parameters, including its resonant frequency, input impedance, return loss ( $S_{11}$ ), and radiation characteristics. By monitoring changes in these parameters, particularly the resonant frequency and reflection coefficient, the presence and magnitude of a stimulus can be quantified.<sup>37</sup>

While antenna geometry defines the electromagnetic mode structure, the choice and processing of functional materials ultimately governs sensor performance by dictating parameters such as conductivity, dielectric permittivity, loss tangent, and mechanical durability. For instance, the conductivity of metallic inks such as silver or copper nanoparticle formulations is determined by appropriate sintering and processing conditions, which in turn regulates the ohmic losses of the antenna structures fabricated with such inks, thereby directly impacting the radiation efficiency, the  $Q$ -factor, the sensitivity, and the limit of detection (LOD) of these antenna structures.<sup>7,10,38</sup> Similarly, polymer substrates (substrates on which the antenna structures are fabricated), such as polyvinylidene fluoride (PVDF) provide mechanical flexibility for strain or vibration sensing applications, but can also introduce detuning effects due to deformation-induced permittivity variations.<sup>39</sup> Textile-based platforms for the antenna structures, while advantageous for their wearability and integration into garments, present porosity and moisture absorption that lead to additional loss pathways and unpredictable permittivity shifts.<sup>40,41</sup> The dielectric permittivity and loss tangent of substrates (such as ceramics, polymers, or nano-composites) govern the resonant frequency and sensitivity of the sensor, making them central parameters in design. For instance, high-permittivity ceramics, such as BaTiO<sub>3</sub>, is an attractive choice of substrate for fabricating miniaturized patch antennas. However, its inherent brittleness and limited flexibility pose challenges for large-scale deployment under practical field conditions.<sup>42</sup>

Equally important are processing methods such as screen-printing, inkjet deposition, extrusion-based 3D printing, and curing conditions, which control the microstructure of the deposited films and thereby influence conductivity, adhesion, and dielectric stability. Thus, the chemistry, processing, and material selection collectively define the electromagnetic response and sensing capabilities of antenna systems, underscoring the need for an integrated materials–device perspective.

The governing equations for patch antenna design and its associated parameters are summarized in Table 1 (notations for the equations are used as follows:  $c$  as the speed of light,  $\epsilon_r$  as the permittivity of the substrate,  $f_r$  is the resonance or operating frequency of the system,  $K_T$  is the temperature sensitivity,  $K_e$  is



Table 1 Patch antenna design parameters and governing equations

Parameters	Related equation
Substrate height ( $h$ )	$h \leq \frac{0.3c}{2\pi f_r \sqrt{\epsilon_r}}$
Patch width ( $W$ )	$W = \frac{c}{2f_r \sqrt{\frac{\epsilon_r + 1}{2}}}$
Effective permittivity ( $\epsilon_{\text{eff}}$ )	$\epsilon_{\text{eff}} = \frac{\epsilon_r + 1}{2} + \frac{\epsilon_r - 1}{2} \left( \frac{1}{\sqrt{1 + 12 \left( \frac{h}{W} \right)}} \right)$
Patch length ( $L$ )	$L = \frac{c}{2f_r \sqrt{\epsilon_{\text{eff}}}} - 0.824h \left( \frac{(\epsilon_{\text{eff}} + 0.3) \left( \frac{W}{h} + 0.264 \right)}{(\epsilon_{\text{eff}} - 0.258) \left( \frac{W}{h} + 0.8 \right)} \right)$
Temperature ( $T$ ) and strain ( $\epsilon$ )	$\frac{\delta f_r}{f_r} = -K_T \delta T - K_\epsilon \epsilon$

the strain sensitivity, *etc.*). These equations, in addition to providing the designing criteria for patch antenna, also account for the influence of different material properties on the antenna performance. For example, these equations clearly indicate that the operating frequency of a patch antenna is strongly influenced by the dielectric permittivity of the medium between the patch and the ground plane. Environmental factors, such as changes in temperature or humidity, alter the effective permittivity,  $\epsilon_{\text{eff}}$  (which also depends on the actual permittivity ( $\epsilon_r$ ), the height ( $h$ ), and the width ( $W$ ) of the substrate) of the substrate, thereby shifting the antenna's operating frequency. This direct correlation between frequency variation and permittivity change enables the designing of the patch antenna to function effectively as a sensor for biomedical, agricultural, and environmental monitoring applications.<sup>7</sup> For strain sensing, two resonant modes, namely the modes in the longitudinal and transverse directions, are typically considered.<sup>43</sup> When a crack forms along the longitudinal direction, the corresponding longitudinal mode experiences a frequency shift, while the transverse mode remains largely unaffected. This distinction provides a reliable means of detecting directional strain. Additionally, patch antennas can operate in a radar-like sensing mode, where radiated waves are tracked through their reflections from a target object. Such a mechanism allows wireless anomaly identification within a system for applications such as breast cancer detection,<sup>44,45</sup> further broadening the antenna's role as a versatile sensing platform. Utilizing these fundamental response behavior of the antennas, over

time, advancements in antenna-based sensors have led to diverse applications. A notable early example was a 1.5 GHz circular patch antenna for high-sensitivity ( $\sim 0.3\%$  resolution) measurement of moisture content in sludge samples.<sup>46</sup> This breakthrough paved the way for using antennas to monitor environmental parameters. Later, antenna-based sensors were integrated with radio frequency identification (RFID) technology for applications like humidity and displacement sensing.<sup>47,48</sup> Temperature sensing was also achieved by leveraging the changes (caused by the temperature) in the dielectric properties of antenna materials.<sup>49</sup> In biomedical sensing applications, variations in tissue dielectric properties can shift the antenna's resonance, enabling non-invasive diagnostics.<sup>50,51</sup> This passive, label-free sensing approach allows for real-time, wireless monitoring and can be adapted for a wide range of applications by appropriate selection of the material and structural design of the antenna. The emergence of printed and flexible electronics has significantly expanded the role of antenna-based sensors, particularly in wearable health monitoring systems.<sup>52</sup> Initially developed for environmental sensing, these antennas are now being adapted for biomedical applications, such as real-time physiological tracking and non-invasive diagnostics.<sup>53,54</sup> As fabrication methods and material technologies continue to evolve, antenna-based sensors are becoming increasingly compact, adaptable, and suitable for integration into next-generation medical, environmental and structural health monitoring devices (Fig. 1). Fig. 2 provides a schematic example of the mechanism of the antenna-based sensing.

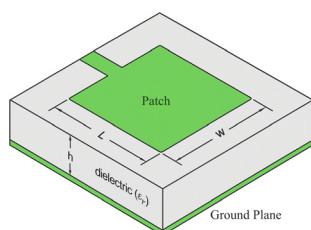


Fig. 1 Patch antenna design.

### 3 Examples of applications of antennas as sensors

#### 3.1 Applications as bio-medical and wearable sensors

In recent times, there has been a massive push to utilize antenna as sensors for bio-medical and wearable electronics applications. Vestrum *et al.*, for example, proposed a patch antenna that was embedded in a diaper, which in turn was



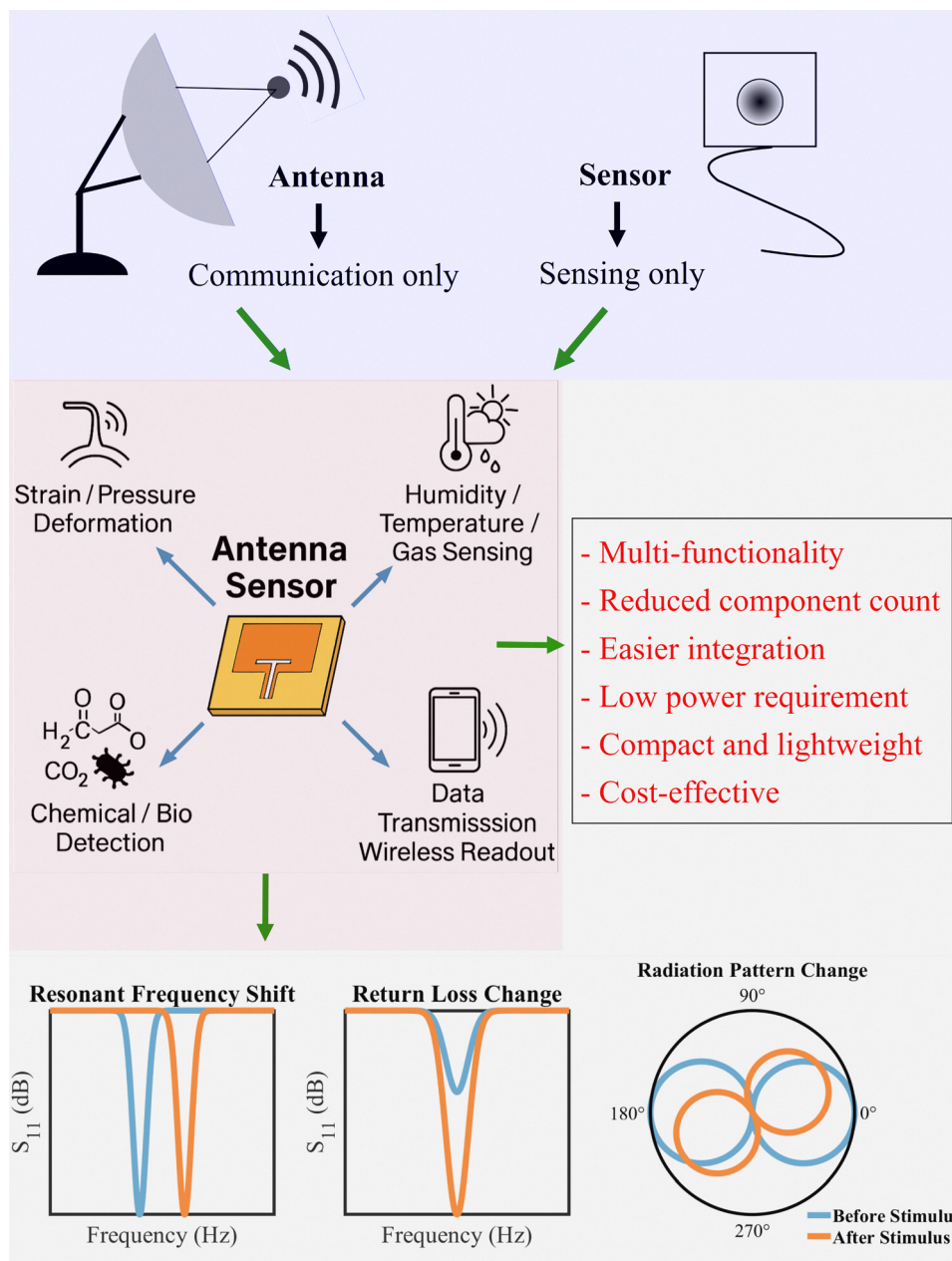


Fig. 2 Concept of antenna based sensing and the corresponding advantages.

integrated with a catheter, in order to monitor de-hydration in real-time.<sup>55</sup> The key sensing mechanism for this study was based on the change in the parametric pattern of the antenna sensor on account of the dehydration-induced conductivity variation of the urine sample. Alsultan *et al.* also explored the ultra high frequency (UHF) radio frequency identification (RFID) technique to sense synthetic euhydrated and dehydrated sweat on different fabrics.<sup>41</sup> Their proposed system classified hydration states with 100% accuracy for liquid concentrations above 50%, ensuring compatibility with the standards of the Federal Communications Commission (FCC) and European Telecommunications Standards Institute (ETSI). For this study, the underlying detection approach relied on identifying distinct patterns in the received signal strength indicator (RSSI) as a

function of frequency. In particular, positive or flat slopes in RSSI were associated with euhydration states, whereas negative slopes corresponded to dehydration states. Lately, they have also developed a low-cost, energy-efficient UHF RFID-based antenna sensor that is capable of remote liquid characterization, addressing key limitations of conventional wireless methods.<sup>56</sup> The sensor incorporated an absorbent within its substrate, allowing the dielectric properties of liquids under test (LUTs) to modulate the tag's read range. This design facilitated much more accurate estimation of relative permittivity and loss tangent as compared to the transmission line method; for example, it demonstrated over 93.5% accuracy (while estimating relative permittivity) and 84% accuracy (while estimating loss tangent), respectively. A study along similar



lines achieved identical accuracy using K-means unsupervised learning when attempting to differentiate between euhydrated and dehydrated sweat in fabrics with concentrations over 58%.<sup>57</sup> Eldamak *et al.* demonstrated a cellulose-based patch antenna (2–4 GHz) (with paper substrate) for non-invasive hydration monitoring using sweat.<sup>58</sup> The key idea of their approach was to leverage the paper substrate as a moisture-absorbing medium, where the absorbed sweat alters the dielectric constant of the paper, thereby enabling hydration sensing. The antenna detected hydration states by monitoring changes in its dielectric properties, which were influenced by the NaCl concentration in the absorbed sweat. There are also examples of several other similar studies where antenna-based sensors were utilized for such hydration and sweat sensing.<sup>40,59–61</sup>

Antenna sensors can also be utilized for detection of tumor and cancer cells.<sup>35,44</sup> Microwave imaging systems identify malignant lesions by detecting dielectric discontinuities in tissues, without exposing patients to ionizing radiation. Low-frequency antenna sensors are used to detect cancerous cells located deep within the body since lower frequencies are suitable for higher penetration depth.<sup>62</sup> In contrast, higher-frequency antenna systems offer improved spatial resolution for superficial tissue imaging, but suffer from increased signal attenuation.<sup>44</sup>

The design and implementation of implantable antennas and sensors form a significant focus within the biomedical research community.<sup>53,63</sup> Ongoing efforts have aimed to develop both components (sensors and antennas) in forms suitable for implantation, with particular interest in integrating antenna functionality with sensing capabilities. Wang *et al.* presented a miniaturized (13.2 mm<sup>3</sup>) implantable antenna sensors, operating at 2.45 GHz in the industrial, scientific, and medical (ISM) band, for breast tumor recurrence diagnosis.<sup>54</sup> The S-shaped monopole antenna sensor demonstrated sensitivity to tissue dielectric changes, with resonance frequency shifts of 9–18 MHz for a permittivity increase of 10. When implanted into the breast tissue, the proposed antenna sensor interacts with the surrounding tissue as a dielectric, forming a capacitance with the antenna. The onset of a tumor significantly changes the tissue permittivity with the permittivity shifting from  $\sim 5$  for normal breast tissue (similar to fat) to values approaching  $\sim 52$  (similar to muscle). These permittivity variations lead to corresponding changes in capacitance and produce a pronounced resonance frequency shift, enabling tumor detection. Simulations and measurements in tissue-mimicking media confirmed its potential for wireless detection of pathological changes. Despite the potential advantages, employing antennas as sensors in biomedical environments remains a huge challenge considering miniaturization, high sensitivity, safety, and efficient communication.<sup>64,65</sup> Nevertheless, successful integration could substantially reduce the complexity and limitations associated with conventional implantable sensor systems.

### 3.2 Applications for structural health monitoring

Structural health monitoring is another sector where antenna sensors have been extensively utilized.<sup>7,66</sup> Recently, Li *et al.* exhibited a miniaturized wireless patch antenna sensor for

sensing structural cracks.<sup>67</sup> They used a high-dielectric Rogers RO3010 substrate to keep the structural footprint low while achieving a high sensitivity ( $\sim 116.1 \text{ MHz mm}^{-1}$ ). The sensor detected crack expansion through relative movements between antenna components and it was possible to conduct wireless interrogation using wide-band antennas. Notably, by exploiting an off-center feeding technique, the sensor exhibited distinct resonant frequencies in both the longitudinal and transverse directions. As a result, crack growth along the longitudinal direction produced a frequency shift only in that axis, while the transverse response remained unchanged, thereby confirming the specific direction of crack propagation. Tchafa *et al.* demonstrated a dual-resonant patch antenna sensor for simultaneous strain and temperature sensing, with frequency shifts linearly correlated to both the parameters (strain and temperature).<sup>43</sup> They also utilized the off-center design technique to decouple the patch length and widthwise resonant frequencies. They formulated the theoretical sensitivity of the system for temperature and strain, and established an opposite relationship between them in transverse direction. Validated through thermo-mechanical testing, the sensor achieved measurement uncertainties of  $0.4 \text{ }^\circ\text{C}$  and  $17.22 \mu\text{e}$ , confirming its potential for multifunctional sensing in a compact design. Daliri *et al.* explored the use of circular microstrip patch antennas for wireless strain sensing, demonstrating a linear relationship between strain and resonant frequency shift. By adopting a meandered design, they achieved a threefold improvement in sensitivity and a fivefold reduction in size as compared to the conventional circular patch.<sup>68</sup> Moreover, this meandered configuration further enhanced the linearity of the strain-frequency response, offering superior performance over the standard circular design. Mohammad *et al.* showed that a single antenna sensor was highly sensitive to crack propagation in the ground plane;<sup>69</sup> however, in order to achieve a large area coverage, a sensor array, which could be formed by multiplexing antenna sensors using frequency division multiplexing given that the crack information was encoded in their resonant frequencies, was necessary.<sup>1</sup> Caizzone *et al.* exhibited a wireless RFID crack width sensor designed for use on materials such as concrete and metal. The sensor was capable of detecting submillimeter deformations.<sup>70</sup> The system consisted of an RFID reader interrogating two closely spaced, strongly coupled RFID tags placed on either side of a crack: this enabled deformation sensing through phase variation in the back-scattered signal under conditions where the distance between the two RFID tags changed (in response to the changes in the crack dimensions). Omer *et al.* developed a crack-depth sensing technique using a passive UHF RFID tag interrogated *via* the ThingMagic M6e platform.<sup>71</sup> By applying power peaks feature extraction (PPFE) and skewness analysis, they were able to achieve high-accuracy crack depth estimation on stainless steel and ferromagnetic samples, with a maximum error of 0.1 mm. Bouzaffour *et al.* developed an embedded autonomous UHF RFID sensor for detecting steel corrosion in concrete, based on the coupling between a dipole antenna and a chloride-exposed steel layer.<sup>72</sup> Quantification in the variations in received signal



strengths enabled detection of thin metallic films, allowing for monitoring of steel mass loss despite moisture interference. A similar type of work, focusing on antenna-based sensing of corrosion in steel and copper, was conducted by Zhang *et al.*<sup>73</sup> and El Masri *et al.*<sup>74</sup>

### 3.3 Applications in agriculture and environment

Antenna-based sensors have emerged as a promising technology for applications in agriculture and in environmental monitoring due to their dual functionality in both sensing and wireless communication. These systems can be designed to passively or semi-passively monitor key environmental parameters such as soil moisture, temperature, humidity, and atmospheric pollutants, facilitating real-time data acquisition over large and often remote areas without reliance on bulky power sources or complex infrastructure.<sup>75–77</sup> Their ability to integrate seamlessly with existing RF communication networks enables cost-effective and scalable deployment for precision agriculture and environmental surveillance. Moreover, the use of antenna-based sensors in regulated frequency bands enhances their compatibility and energy efficiency, making them particularly suitable for long-term field monitoring under diverse environmental conditions. For example, Yao *et al.* showed that temperature sensing without electronics could be achieved *via* wireless interrogation of passive antenna sensors by utilizing an ultra-wideband microstrip antenna as the transmitter/receiver and a microstrip patch antenna as the sensing element.<sup>78</sup> They derived the thermal sensitivity of the system by accounting for the substrate's coefficient of thermal expansion and the temperature-dependence of the dielectric constant, thereby establishing a clear linear relationship between temperature variation and resonant frequency shift. Borgese *et al.* presented a chipless RFID humidity sensor based on a finite artificial impedance surface with three concentric loops, enabling high-*Q* resonance peaks.<sup>79</sup> They used a thin sheet of NB-TP-3GU100 Mitsubishi paper substrate coated with humidity-sensitive ink acting as the chemically interactive material (CIM). Changes in humidity altered its permittivity, shifting the resonance nulls in the sensor's frequency response, which were used to estimate relative humidity. Maximum sensitivity was achieved when the resonators directly contacted the CIM, avoiding air gaps. Fabricated *via* low-cost inkjet printing, the sensor encoded relative humidity data through frequency shifts of up to 270 MHz across 50–90% RH. Recently, Liu *et al.* proposed a novel reconfigurable four-port antenna-based sensor with multi-parameter characteristics.<sup>80</sup> They were able to achieve a passive, reusable sensor array integrating multiple sensitive materials enabling a long-term, power-free monitoring of parameters like humidity and pH, suitable for critical environments. In the proposed chipless radio frequency identification (CRFID) sensing system, the tag operated as a multiresonant circuit coated with functionalized materials whose dielectric properties varied with changes in the environmental conditions. These variations shifted the tag's resonant frequency, which was captured by the reader antennas through *S*-parameter changes, enabling multiparameter sensing. Cross-

polarized antenna configurations further improved signal robustness by reducing mutual interference. The system demonstrated strong potential for future precision agriculture applications. Lately, another study has been conducted to investigate how soil water content and antenna positioning affect the performance of monopole antennas used in such systems.<sup>81</sup> Numerical and experimental results across twelve scenarios showed that while antenna performance remained stable for half the number of cases, significant losses in radiation efficiency and bandwidth occurred under specific conditions, thereby highlighting the importance of considering environmental factors when designing antenna systems for internet of things (IoT)-driven agriculture. Rahman *et al.* presented a compact microwave sensor with a circular radiating patch and semi-circular slots, designed for detecting salinity and sugar concentration.<sup>82</sup> The fabricated sensor functioned on the basis of changes in reflection coefficient due to variations in dielectric constant. Simulations performed using high frequency simulation software (HFSS) and experiments confirmed the sensor's sensitivity to salt and sugar levels, demonstrating its effectiveness for concentration monitoring. Kazemi *et al.* presented a  $\text{Ti}_3\text{C}_2\text{T}_x$  MXene-based antenna sensor for wireless detection of volatile organic compounds (VOCs) and humidity.<sup>83</sup> Their proposed sensor could detect different humidity concentrations ranging between  $77.8 \pm 2\%$  to  $94 \pm 1\%$  and the exposure of the antennas to the VOCs caused an upshift in the operating frequency of the antenna sensor. The underlying mechanism of the system for sensing the VOCs relied on gas adsorption at  $\text{Ti}_3\text{C}_2\text{T}_x$  MXene's functional groups and structural defects, which induced local bond deformations (*e.g.*, Ti–O) and modulated electrical conductivity. These conductivity changes increased resistivity, observed as a resonant frequency shift in the transmission response ( $S_{21}$ ). The MXene antenna sensor also exhibited a large frequency shift at high humidity due to water molecule penetration between MXene flakes, which increased the interlayer spacing and membrane resistivity. This change in conductivity manifested as a resonant frequency ( $S_{21}$ ) shift in the transmission response. Bouchalkha *et al.* demonstrated a planar microstrip antenna sensor capable of detecting pH levels in small liquid volumes using RF signal shifts.<sup>84</sup> The sensor detected changes in dielectric constant from solution droplets on its surface, producing measurable resonance frequency shifts in the recorded microwave response. The sensor demonstrated a 180 MHz frequency shift between pH 3 and pH 10, with high sensitivity, reusability, and a strong polynomial correlation ( $R^2 = 92.16\%$ ), making it suitable for real-time pH monitoring applications. There have been also a few related studies on soil moisture and grain moisture content estimation using antenna based sensors.<sup>85–87</sup>

### 3.4 Applications in automotive, aero-space, and defense

Antenna-based sensors also play a critical role in auto, aero-space and defense industries, offering compact, lightweight, reconfigurable and multifunctional capabilities essential for advanced sensing and improved communications.<sup>88–90</sup> In aero-space applications, these sensors are employed for structural



health monitoring of aircraft components, enabling real-time detection of strain, cracks, and temperature variations to enhance safety and maintain efficiency. Radar sensors are essential components in both the automotive and aerospace industries, enabling advanced safety features, precise navigation, and autonomous operations. It is a well-known fact that the radar sensors operate by transmitting electromagnetic waves and analyzing the reflected signals from objects. By measuring the time delay, frequency shift (Doppler effect), and amplitude of the returned signal, radar sensors can determine the distance, velocity, angle, and size of a target.<sup>91</sup> In the automotive sector, they support features such as advanced driver-assistance systems (ADAS) and autonomous driving functions, adaptive cruise control, collision avoidance, blind spot monitoring, and parking assistance by providing reliable object detections and distance measurements under diverse environmental conditions.<sup>92</sup> Similarly, in aerospace applications, radar sensors are used for terrain mapping, obstacle avoidance, weather monitoring, and autonomous landing systems, offering high-resolution data regardless of visibility.<sup>93</sup> Their robustness, real-time responsiveness, and performance in adverse conditions make radars indispensable for enhancing safety and autonomy across both industries. In defense, antenna sensors are integrated into radar systems, unmanned aerial vehicles (UAVs), and wearable soldier technologies for secure communication, environmental sensing, and situational awareness.<sup>94,95</sup> Their ability to operate in harsh environments, coupled with passive or semi-passive functionality, makes them highly suitable for long-term deployment in mission-critical scenarios, contributing to improved system reliability and operational readiness.

### 3.5 Miscellaneous applications

Antenna sensors play a pivotal role in Internet of Things (IoT) and outer space applications due to their ability to enable wireless, real-time, and energy-efficient sensing. In IoT systems, antenna sensors are embedded into smart devices and environments to monitor variables such as temperature, humidity, pressure, and mechanical deformation.<sup>96–99</sup> Their passive or semi-passive nature, often leveraging RFID technology, allows for low-cost, battery-free operation, which is essential for scalable and long-term deployment in smart cities, industrial automation, and healthcare monitoring. In outer space applications, antenna sensors are used for structural health monitoring of spacecraft, satellites, and space stations. Ultrahigh frequency (UHF) wireless passive antenna sensors are also now being leveraged as food spoilage indicator and to monitor food quality indices.<sup>15,100,101</sup> For instance, in ref. 101, the authors used an interdigitated capacitor coated with polyaniline (PANI) that selectively reacted with ammonia, causing measurable changes in capacitance or resistance. These changes were digitized by a low-power passive circuit integrated with an RFID antenna, allowing the sensor to wirelessly transmit both ammonia concentration and identification data to a reader for real-time food quality monitoring. Overall, antenna sensors provide critical data on strain, thermal variations, and impact events in

harsh environments without the need for wired connections, thereby reducing system weight and complexity. Their robustness, radiation resistance, and ability to function in vacuum conditions make them ideal for aerospace missions, where reliability and minimal maintenance are paramount.<sup>102</sup> Thus, the use of antenna-based sensors in extreme conditions, such as elevated altitudes and submerged settings, is an area of growing interest. These applications hold considerable potential for enhancing wireless communication in domains that require resilient performance, including satellite-based environmental observation, unmanned vehicle operations, and subsea resource exploration.<sup>103–106</sup> Some prominent examples of antenna based sensors covering these different discussed applications have been listed in Table 2.

## 4 Limitations

Although antenna-based sensors offer significant advantages in terms of wireless operability and multifunctionality, they suffer from several limitations that have often impeded their broader applicability.<sup>7,108</sup> In this section, we highlight some of these key limitations. A key challenge/limitation is signal attenuation and detuning, in the presence of unfavorable surrounding environment. For example, the presence of lossy media such as biological tissue, soil, concrete, *etc.* attenuate electromagnetic waves, while nearby materials or human proximity may shift the resonant frequency and reduce sensing accuracy.<sup>109</sup> Power constraints also remain critical, since passive sensors typically exhibit limited readout range due to low radiation efficiency and restricted power handling, whereas active systems increase energy consumption and compromise long-term autonomy.<sup>110</sup>

Mechanical deformation presents another source of limitation, especially in strain-sensitive designs. While flexible and stretchable polymers or textile substrates enable compliance, they also introduce detuning effects and geometric instability.<sup>1</sup> Embroidered antennas, for instance, provide higher stretchability than metallic inlays but suffer from the low resolution of yarn stitches, making fine geometrical features impractical. Moreover, stretching alters both the substrate and the conductive path, causing nonlinear responses and reducing reproducibility over time.<sup>111</sup> Repeated mechanical loading further accelerates material fatigue, thereby reducing long-term reliability.

Furthermore, the ongoing drive toward achieving miniaturization, while critical for wearable, implantable, and portable applications, inevitably introduces trade-offs in terms of antenna properties.<sup>112</sup> The miniaturized designs often reduce bandwidth, sensitivity, and radiation efficiency, and also increases susceptibility to fabrication tolerances. Achieving reliable performances in miniaturized antennas thus remains a persistent bottleneck. At the same time, cost and scalability also limit broader adoption. High-frequency and high-performance sensors often require specialized inks, nanocomposites, or engineered substrates, along with precision



Table 2 Examples of recently developed antenna sensors for different area of applications

Area of applications	Sensing properties	Antenna type/design/structure	Fabrication technique	Materials used	Sensing parameters	Operating frequency/sensitivity/range/accuracy	Year and references
Bio-medical and wearables	Hydration level	Patch	Copper patch adhered on top of the substrate	Substrate: Rogers RT/dur-oid 5880; Patch: copper	S-parameters	Sensing range: electrolyte concentration in urine sample from 2.5% (hydrated) to 5.0% (dehydrated)	2023 <sup>55</sup>
		Patch	Used adhesive spray	Substrate: denim, cotton, polyester; patch: copper	Power transmission co-efficient	Sensing range: electrolyte concentration more than 50% in sweat sample (with 100% accuracy)	2025 <sup>41</sup>
		Slotted rectangular patch	Copper patch adhered on top of the substrate	Substrate: cellulose filter paper; patch: copper	S-parameters	Sensing range: NaCl concentrations in sweat (2–4) GHz	2018 <sup>58</sup>
Structural health monitoring		Metallic reader tag	Commercial grade tag	Substrate: earlobe	Di-electric permittivity	Operational range: (0.9–1) GHz; sensitivity: ~120 KHz shift for a 1% change in dehydration	2024 <sup>59</sup>
		Software driven radio-transmission (non-contact based)	Used commercial grade transceiver	RF transceiver	Orthogonal frequency division multiplexing (OFDM)	Accuracy: 93.8%	2023 <sup>61</sup>
	Sucrose content	Textile UHF-RFID tag	Adhesive and embroidered with conductive yarn	Substrate: polyester fibers; UHF-RFID integrated circuit (IC) chip	S-parameters	Operational range: (865–868) MHz	2021 <sup>40</sup>
	Breast cancer detection	Metal based (array) semi-circular multi-static radar architecture	—	Breast tissue as di-electric;	Di-electric property	Central frequency 33.25 GHz; bandwidth ~13.5 GHz	2017 <sup>44</sup>
	Crack sensing	Rectangular patch	Copper patch adhered on top of the substrate	Substrate: Rogers RO3010; patch: copper	S-parameters	Sensitivity: ~116.1 MHz mm <sup>-1</sup>	2024 <sup>67</sup>
	Strain and temperature	Patch	Print-etching technique	Substrate: Rogers RT/dur-oid 5880; patch: copper	S-parameters	Up to 100 °C	2018, <sup>43</sup>
	Strain and humidity	Dipole	Print-etching technique	Substrate: polyamide; patch: copper	S-parameters	Sensitivity: 24.03 kHz per $\mu\text{e}$ ; 12.38 MHz per %RH	2022 <sup>107</sup>
	Crack depth	UHF RFID tag	Commercial grade tag used	UHF-RFID tag interrogated by ThinkMagic M6e	Received signal strength indicator (RSSI)	Operational range: (902–928) MHz	2018 <sup>71</sup>
	Corrosion detection	UHF RFID tag	Commercial grade chip used	UHF-RFID integrated chip	Received signal strength indicator (RSSI)	Sensitivity: depth more than 1 $\mu\text{m}$	2021 <sup>72</sup>
	Agriculture and environment	Humidity and pH level	Chipless radio frequency identification (CRFID)	Copper patch adhered on top of the substrate	Substrate: Rogers RO3003; patch: metal based microstrip	S-parameters	Sensing range: (50–80) %RH, (4–7) pH; sensitivity: ~1.08 MHz per %RH
Soil moisture		Reconfigurable complementary spiral resonator	Copper patch adhered on top of the substrate	Substrate: Rogers RO4003C; patch: copper	S-parameters	Operating frequency shifts around 20 MHz for change in permittivity from 1 to 20	2023 <sup>77</sup>
Soil water content		Monopole	—	Substrate: poly(lactic acid (PLA) and foam board; patch: copper	S-parameters and radiation efficiency	Operational range: (1.83–4.2) GHz	2024 <sup>81</sup>
Automotive, aerospace and defense	Salinity and sugar concentration	Slotted circular patch	Copper patch adhered on top of the substrate	Substrate: FR4; patch: copper	S-parameters	Operational range: (3.92–5.5) GHz	2019 <sup>82</sup>
	VOC and humidity	Circular patch	Fabricated $\text{Ti}_3\text{C}_2\text{T}_x$ patch adhered on top of the substrate	Substrate: Rogers 6010; patch: $\text{Ti}_3\text{C}_2\text{T}_x$	S-parameters	Sensing range: (77.8–94.1) %RH, VOC (8–80) parts per thousand	2022 <sup>83</sup>
	Radar sensing	Millimeter wave antennas	Computer numerical control (CNC)	Aluminum	S-parameters and gain	Operational range: 77 GHz	2025 <sup>89</sup>
	Reconfigurable multiple input multiple output (MIMO) structure	—	Substrate: RT Duroid 5880; patch: metal	S-parameters and gain	Operational range: (23.8–24.3) GHz	2025 <sup>90</sup>	





Table 2 (continued)

Area of applications	Sensing properties	Antenna type/design/structure	Fabrication technique	Materials used	Sensing parameters	Operating frequency/sensitivity/range/accuracy	Year and references
Miscellaneous	Hand gesture recognition for visually impaired Ammonia sensing for food quality investigation	Frequency modulated continuous wave millimeter wave radar RFID tag	— Micro-fabrication (lithography)	Commercial grade radar sensor Patch: polyamine covered copper substrate: Rogers XT/Duroid 8000	Range and velocity information Capacitance and resistance change	Accuracy: 97.1% Sensing range: 3 ppm (minimum) of ammonia	2025 <sup>99</sup> 2020 <sup>101</sup>

manufacturing techniques: all of these factors drive up costs and hinder mass production. Long-term biocompatibility for biomedical sensors and compliance with spectrum regulations further complicate real-world deployment.

Fabrication of flexible antenna sensors also faces several challenges. For instance, screen-printing techniques, which are often used for antenna fabrication, are constrained by a limited number of realizable layers, inadequate control over the conductive layer thickness, and relatively low printing resolution.<sup>3</sup> These limitations restrict the broader applicability of the antenna structures (fabricated with screen printing techniques) as wearables, given that the wearable systems demand higher fabrication precision for reliable communication. Other widely utilized techniques (*e.g.*, inkjet printing or micro-fabrication) used for fabricating antenna structures can encounter adhesion issues between the patch and the substrate under harsh environmental conditions.

Environmental durability presents an additional concern, as factors such as humidity, temperature variations, chemical exposure, and mechanical stress can compromise antenna structural integrity and degrade performance over time—issues particularly pronounced in flexible or non-metallic substrates.<sup>113</sup> From a practical standpoint, fabrication and cost considerations also play a limiting role. Achieving reproducible and high-frequency antenna designs often demand specialized materials and high-precision processes, which reduce scalability and raise manufacturing costs.

While emerging avenues such as 3D and 4D printing, coupled with machine learning (ML), artificial intelligence (AI)-based self-calibration, and adaptive algorithms have been proposed to mitigate some of these issues (discussed in the following sections), such approaches introduce new dependencies on data availability, computational resources, and algorithm robustness.<sup>35</sup> In addition, external challenges such as electromagnetic interference in crowded wireless environments, the lack of standardized frameworks for interoperability, spectrum regulations, and long-term bio-compatibility in biomedical contexts further restrict the deployment of antenna-based sensors. Overcoming these obstacles is essential for enabling the reliable integration of antenna-based sensors into everyday applications.<sup>112</sup>

## 5 Next generation sensor antennas: utilizing the power of 3D printing and machine learning

Leveraging advanced materials (*i.e.*, materials that can be engineered to make them 3D printable and attribute them with specific functionalities) such as conductive composites, conductive polymers, hydrogels, elastomers, conductive nanomaterial-based inks, *etc.*, 3D printing has revolutionized the fabrication of complex geometries of efficient and multi-functional devices. Unlike conventional microfabrication techniques, 3D printing allows direct and autonomous fabrication of intricate functional designs onto various substrates without

the need for elaborate preprocessing facilities. Sensor antennas fabricated using existing 3D printing technologies are gaining prominent recognition as next-generation devices due to their exceptional properties such as stretchability, enhanced flexibility, ultra thin profiles, biocompatibility, and lightweight nature. Fig. 3 summarizes the key usefulness of utilizing 3D printing over conventional fabrication processes, with regards to wearable antenna-based sensors, where such flexibility, stretchability, *etc.*, become critical.

Moreover, the integration of machine learning (ML) into the design and development process further advances the capabilities of sensor antennas, fabricated by both traditional and 3D printing methods. ML algorithms are increasingly employed to predict antenna performance, optimize geometries, and accelerate the exploration of design structures. Such ML-based approaches are significant improvements over conventional trial-and-error approaches, which require substantial time, expert intervention, and computational resources. The ML approaches, on the contrary, first gather the performance data from antenna models or measurements and emphasize critical metrics such as radiation pattern, gain, frequency, and bandwidth. The data is then used to build an ML model that determines how the different design parameters affect the antenna-based sensor's performance. Once the model is trained, the model aids in antenna design optimization by predicting results across multiple configurations, and further verification is used to confirm fulfillment of the required performance objectives. This paradigm shift allows for more intelligent, efficient, and targeted design strategies that meet the growing demands for high performance, multifunctionality, and adaptability in modern communication systems.<sup>122</sup> Fig. 4 summarizes the key usefulness of utilizing machine

learning for optimizing designs for the antenna-based sensors for ideal performances.

### 5.1 Next-generation sensor antenna for healthcare systems

In a study by Ashish *et al.*, recent progress in the development of state-of-the-art 3D printed wearable biosensors<sup>123</sup> has been reviewed. This review paper, in addition to focusing on three primary printing processes, namely vat photopolymerization, material jetting, and material extrusion that are used for the purpose, clearly identified the different types of 3D printed biosensor devices, such as wearable oximeters,<sup>124</sup> glucose monitors,<sup>125</sup> lactate and sweat detectors,<sup>126</sup> strain and tactile sensors,<sup>127</sup> artificial skin,<sup>128</sup> electronic tattoo sensors<sup>129</sup> and EEG (electroencephalogram) and ECG (electrocardiogram) devices.<sup>130</sup> A separate paper<sup>131</sup> critically reviewed the significance of material suitability for the deployability and uses of printed electronics in neurotechnology. This review paper stressed on the importance of selecting biocompatible, flexible, and electrically suitable materials, while signifying how conductive inks based on metallic nanoparticles (*e.g.*, gold, silver, platinum), conducting polymers (*e.g.*, PEDOT:PSS, PANi, PPy), and carbon nanomaterials (*e.g.*, CNTs, graphene) play a pivotal role in dictating the device performance. One study focused on continuous glucose monitoring (CGM) with a sensor antenna that was positioned above the pancreas and could capture dielectric radiation signals non-invasively. The research identified the pancreas as the optimal location for CGM based on the performance of the proposed H-shaped I-slot (HSIS) patch antenna. This HSIS antenna functioned as a sensor by detecting variations in the dielectric properties and transmitting signals that reflected the glucose levels, thereby enabling the monitoring of the glucose levels.<sup>132</sup> Another study adopted the same

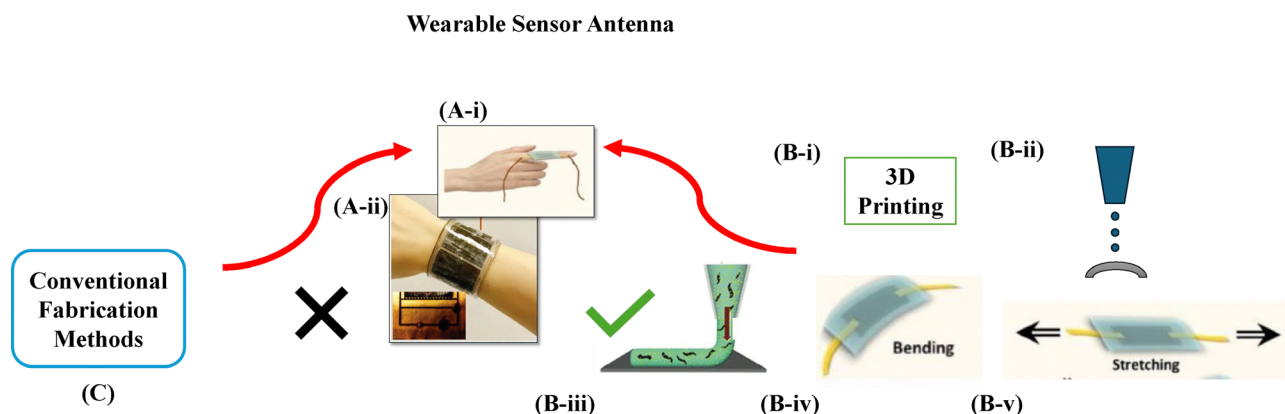


**Fig. 3** Achieving wearable sensor antenna as (A-i) finger mount and (A-ii) wrist mount. Parts (A-i) and (A-ii) have been reproduced from ref. 114 [W. Y. Ko, L.-T. Huang and K.-J. Lin, Green technique solvent-free fabrication of silver nanoparticle–carbon nanotube flexible films for wearable sensors, *Sens. Actuators, A*, 2021, **317**, 112437] and ref. 115 [Y. Zhu, J. Qin, G. Shi, C. Sun, M. Ingram, S. Qian, J. Lu, S. Zhang and Y. L. Zhong, A focus review on 3D printing of wearable energy storage devices, *Carbon Energy*, 2022, **4**, 1242–1261], respectively. (B-i) Schematic showing that 3D printing can fabricate such wearable sensor antenna with the 3D printing method being (B-ii) droplet-based printing (like inkjet or aerosol jet printing) and (B-iii) syringe printing. Such 3D printing is useful for wearable sensor antenna as these printing methods can print on bendable [see (B-iv)] and stretchable [see (B-v)] substrates. Part (B-iii) has been reproduced from ref. 115 [Y. Zhu, J. Qin, G. Shi, C. Sun, M. Ingram, S. Qian, J. Lu, S. Zhang and Y. L. Zhong, A focus review on 3D printing of wearable energy storage devices, *Carbon Energy*, 2022, **4**, 1242–1261], while parts (B-iv) and (B-v) have been reproduced from ref. 114 [W. Y. Ko, L.-T. Huang and K.-J. Lin, Green technique solvent-free fabrication of silver nanoparticle–carbon nanotube flexible films for wearable sensors, *Sens. Actuators, A*, 2021, **317**, 112437]. (C) Identification of the inability of the conventional fabrication methods to fabricate such wearable sensor antenna.



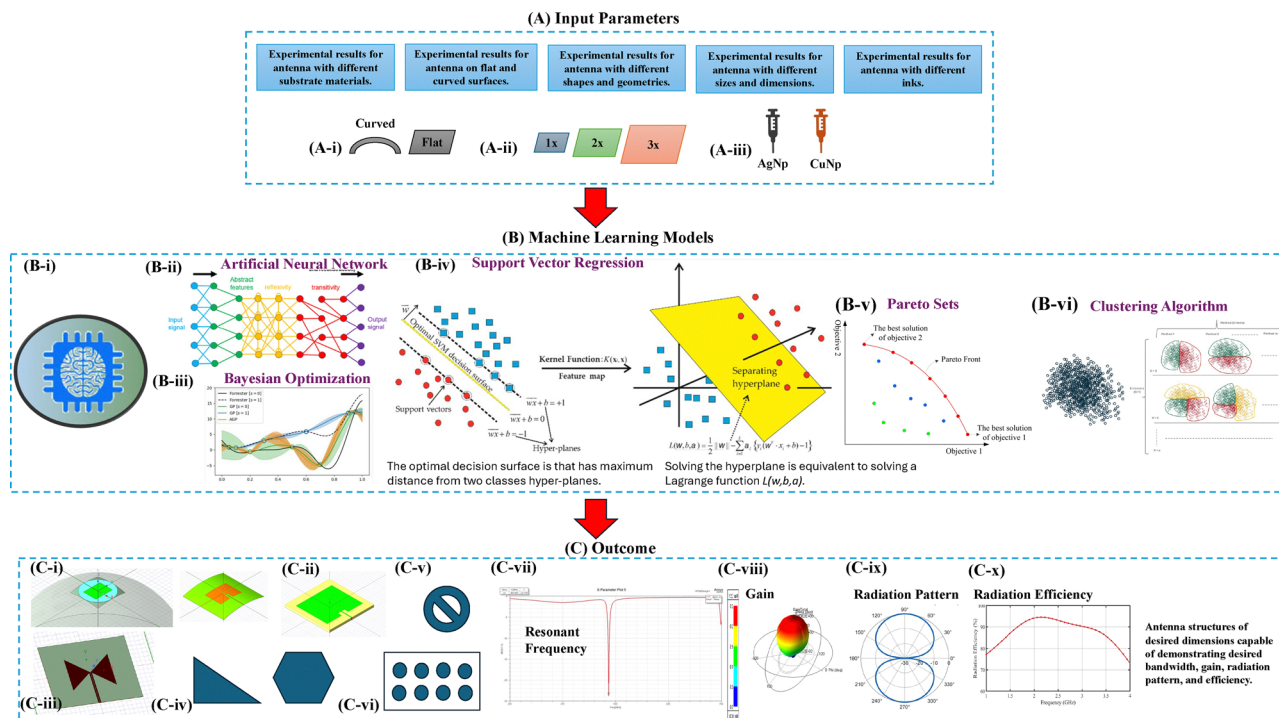


**Fig. 4** (A) Input parameters for developing the ML model for optimizing the parameters that ensure the best performance of the antennae-based sensors. These parameters are obtained from different experiments (as shown) that will be performed to generate a sufficient amount of the input data. This will involve generating experimental data on antenna performance on flat and curved surfaces [see (A-i)], on antenna performances on substrates of different dimensions [see (A-ii)], and on antennae fabricated (3D printed) with different types of inks, namely silver nanoparticle (AgNp) based inks and copper nanoparticle (CuNp) based inks [see (A-iii)]. (B) Different machine learning models [(B-i)] that will be developed using the information from the initial experiments. These models include [(B-ii)] artificial neural network, [(B-iii)] Bayesian optimization, [(B-iv)] support vector regression, [(B-v)] Pareto sets, [(B-vi)] clustering, etc. Parts (B-i), (B-ii), (B-iii), (B-iv), (B-v), and (B-vi) have been reproduced from ref. 116 [A. Singh, B. Mandal, B. Biswas, S. Chatterjee, S. Banerjee, D. Mitra and R. Augustine, *Microwave Antenna-Assisted Machine Learning: A Paradigm Shift in Non-Invasive Brain Hemorrhage Detection*, *IEEE Access*, 2024, **12**, 37179–37191.], ref. 117 [A. Nicolle, S. Deng, M. Ihme, N. Kuzhagaliyeva, E. A. Ibrahim and A. Farooq, *Mixtures Recomposition by Neural Nets: A Multidisciplinary Overview*, *J. Chem. Inf. Model.*, 2020, **64**, 597–620; Copyright 2020 American Chemical Society], ref. 118 [A. Sabbatella, A. Ponti, A. Candelieri and F. Archetti, *Bayesian Optimization Using Simulation-Based Multiple Information Sources over Combinatorial Structures*, *Mach. Learn. Knowl. Extr.*, 2024, **6**, 2232], ref. 119 [D. Wang, J. Peng, Q. Yu, Y. Chen and H. Yu, *Support Vector Machine Algorithm for Automatically Identifying Depositional Microfacies Using Well Logs*, *Sustainability*, 2019, **11**, 1919], ref. 120 [L. Yang, A. Zhu, J. Shao and T. Chi, *A Knowledge-Informed and Pareto-Based Artificial Bee Colony Optimization Algorithm for Multi-Objective Land-Use Allocation*, *ISPRS Int. J. Geo-Inf.*, 2018, **7**, 63], and ref. 121 [S. F. Pileggi, *Clustering with Uncertainty: A Literature Review to Address a Cross-Domain Perspective*, *Informatics*, 2025, **12**, 38], respectively. (C) Outcome from the ML model: optimization of the antenna structure (for sensor applications) in terms of fabricating either (C-i) rectangular curved patch antenna, (C-ii) rectangular flat patch antenna, and (C-iii) bow-tie antenna. Also, in terms of the patch antenna, the optimized structure might be (C-iv) triangular or polygonal, (C-v) one with slots, and (C-vi) one with arrays. The outcome will be characterized in terms of the performance parameters of the designed antenna. These parameters are (C-vii) resonant frequency, (C-viii) gain, (C-ix) radiation pattern, and (C-x) radiation efficiency.

approach of non-invasive monitoring by using machine learning (ML) to detect the dielectric changes in the brain.<sup>116</sup> In this study, a two-antenna system was positioned above the head to successfully determine the exact locations of the brain hemorrhage using ML classifiers.

Both the academic and the industrial sectors are leveraging the stretchability and the foldability of 3D-printed sensor antennas for integrating them into wearable and flexible electronic systems. These critical characteristics (stretchability and foldability) are essential to ensure robust device performance under repeated deformation, bending, and stretching during real-world use. In a recent paper, the authors used multi-material one-step extrusion printing to simultaneously deposit a cellular bioink (cardiac cells in ECM hydrogel), a conductive bioink (graphite flakes in PDMS), and a dielectric/passivation bioink (PDMS with surfactant) to fabricate heart patches.<sup>131</sup>

The one-step 3D printed heart patch was soft, flexible, and robust, capable of withstanding continuous mechanical deformations, such as stretching and twisting, which imitated the dynamic nature of the contracting heart. In another recent study, an ML-based human activity recognition (HAR) system was combined with advances in miniaturized wearable antennas. The flexible mosaic antenna collected radio signal data at various activity levels using recurrent neural networks (RNNs) with long short-term memory (LSTM) cells to categorize human activities from time-series signals. This design approach surpassed other antenna designs in efficiency, size, and signal degradation with high customization and scalability as well as lower cost.<sup>133</sup>

Biomedical sensor antennas, despite their potential for improved health monitoring, have considerable technological challenges. Specific absorption rate (SAR) requirements are



especially stringent,<sup>134,135</sup> requiring antenna designers to decide between radiative efficiency and safety. Clinical designs usually have to maintain SAR values far lower than the regulatory limitations, especially for implanted devices, where the dielectric properties of the tissues that surround these devices are typically high and have a significant impact on how electromagnetic radiation interacts causing an immense effect on antenna performance as well as energy absorption.<sup>136–138</sup>

3D-printed antenna structures designed as implants can suffer from various challenges. For example, many printed polymers (used for 3D-printing of antenna structures) may contain residual monomers, additives, or curing byproducts with unknown long-term biological effects. Furthermore, the layer-by-layer printing processes can result in surface porosity and microstructural defects. All these factors might trigger adverse reactions with the antenna structures interacting with the surrounding tissues or might allow ingress of bodily fluids into the implanted antenna structures endangering the device stability and safety.<sup>139</sup> To address these challenges, printed antennas require encapsulations made from biocompatible materials; however, such encapsulations can alter electromagnetic performance by shifting resonant frequencies and affecting antenna efficiency, while inducing impedance mismatches and increasing insertion losses, resulting in gain reductions.<sup>140</sup>

Dynamic 4D-printed structures further complicate system calibration due to material swelling and stimuli-responsiveness of the smart materials.<sup>140</sup> As reported in ref. 141 the bendability of the ink-jet printed antenna can induce frequency changes of several hundred MHz, necessitating adaptive recalibration during operation to reduce sensor cross-sensitivity. Machine learning approaches intended for automatic system calibration and drift compensation remain constrained by a lack of available large multi-patient datasets; reported *k*-nearest neighbor (*k*NN) and random forest models show root mean square (RMS) error reductions on simulated datasets, but performance might decline in the presence of high physiological noise, nonstationary tissue properties, or variable external electromagnetic environments.<sup>137,142,143</sup> A critical impact of these constraints is the reduction in radiation efficiency and gain of biomedical antennas.

## 5.2 Data-driven and additive manufacturing approaches in space applications of antenna sensors

Space exploration is being revolutionized by incorporating machine learning (ML) and deep learning (DL) techniques that significantly reduce development cycles and allow satellites to navigate tasks without human intervention. A recent study proposed a deep bidirectional long-short term memory network (DBLSTM) for space sensor antennas to monitor the integrity of satellite structures. The purpose of the proposed system was to identify and examine how sensitively the sensor can point out the structural damages of an orbiting satellite. For this purpose, time-series data was processed and the ML algorithm was effectively trained and tested to recognize different levels of structural damage.<sup>144</sup> In a review by Soumya *et al.* the use of machine learning (ML) and deep learning (DL) techniques were

extensively reviewed for the mm-wave radar sensing across a variety of domains, including space-related applications. Specifically, ML and DL were applied to radar signal processing for object detection, classification, tracking, and segmentation by learning from radar intermediate-frequency (IF) data and radar-generated images (such as range-angle and range-Doppler maps). Additionally, it is considered that one can combine ML models such as random forests and graph neural networks with mm-wave radar data for future improvements in space exploration missions and for advancing applications under challenging conditions.<sup>145</sup>

Additionally, extensive deployment of 3D printing has enabled space industry to test the boundaries for human exploration. In a recent review, Peverini *et al.* noted that metal-based selective laser melting (SLM) and direct metal laser sintering (DMLS) are the most adopted 3D printing techniques for radio frequency (RF) components,<sup>146</sup> while other printing methods such as fused deposition modeling (FDM) and stereolithography (SLA) are also important. In the work of Teniente *et al.*, the authors compared the RF performance of 3D printed compact spline horn antennas (as a part of a direct radiating array for SatCom) against their traditionally manufactured counterparts.<sup>147</sup> In this paper, the 3D printing approach employed to fabricate the antennas was SLA, in which the components were further metallized with copper. Notably, in another study,<sup>148</sup> a 3D-printed ABS antenna for plastic CubeSats was successfully fabricated directly onto a curved surface, demonstrating the process versatility for complex geometries. In this study, a significant size reduction was achieved without affecting the uplink and downlink S-band frequencies.

## 5.3 Data-driven and additive manufacturing approaches for adaptive antenna manufacturing for automotive sensing

3D printing has garnered significant interest from the automotive industry for next-generation vehicles. Therefore, the automotive industry is moving beyond using 3D printing solely for body panels and structural components. The number of sensors in modern vehicles has surged, including radars, cameras, LiDAR systems, and ultrasonic parking aids that feature numerous antennas operating across a wide range of frequency bands.<sup>149</sup> However, integrating these components remains labor-intensive and is often an afterthought in the design process. Gjokaj *et al.* employed stereolithography for integrating antennas and sensors directly onto large, non-planar 3D printed plastic structures, such as automotive bumpers.<sup>149</sup> In another study, antenna-based sensor was developed for proposing a smart parking space detection system for urban environments in order to help drivers quickly locate free spaces and to assist administrators manage parking and billing.<sup>150</sup> Specifically, a 3D-printed dual-mode detection approach was developed, where a magnetic sensor was used for initial detection and a high-gain antenna at K-band (24–24.25 GHz) radar was employed for confirmation to avoid a false detection result. For W-band automotive radar applications (75–82 GHz), a 3D printed (using SLA) slotted waveguide



array (SWA) antenna was specially developed for performing in extended wavelength range.<sup>151</sup> Integrating sensors and antennas in automotive systems are becoming more critical, extending to radar sensors for automatic driving. Featured in a related study by Mohan *et al.*, heating coils were fabricated using several 3D printed techniques such as fused deposition modeling (FDM) and contactless inkjet dispensing onto the radome (sensor housing), thereby significantly simplifying the manufacturing process and minimizing the number of required components.<sup>152</sup> The heating coils were used for de-icing to ensure reliable operation in winter conditions for advanced driver-assistance systems (ADAS) such as cruise control, collision warning, and emergency braking.

Current research emphasizes the use of deep learning models over trial-and-error approaches or computationally expensive simulations as a more efficient approach to the design process. A recent review investigated the major breakthroughs in automotive radar technology enabled *via* the integration of deep learning algorithms.<sup>153</sup> For example, super-resolution direction-of-arrival (DOA) estimation outperformed typical hardware-based techniques such as 3D-printed antenna arrays by successfully identifying closely placed cars from a single photo after training on many datasets. This software-driven method provided a strong alternative to hardware scaling, thereby improving radar performance for safer and more dependable autonomous systems.<sup>153</sup> Moreover, the work of Schüßler *et al.* explored a novel approach for enhancing automotive radar images by training a deep neural network (DNN) solely on synthetic data generated from a virtual radar sensor that closely mimicked a real automotive MIMO radar.<sup>154</sup> The key innovation was the use of an advanced virtual sensor, which simulated a radar with superior performance to provide ground truth data for training the DNN to learn to transform noisy, low-resolution input images into high-quality, clutter-free outputs without requiring manual annotation. The trained DNN not only drastically decreased noise and clutter, but it also sharpened pictures and minimized sidelobes, resulting in better simulated and real-world radar readings.<sup>154</sup>

#### 5.4 Additive manufacturing and machine learning for integrated sensing systems for structural health and environmental monitoring

3D printing of sensor antennas spans a wide range of applications not only limited to applications in healthcare systems, space and defense, and automotive industries. The applications also extend to diverse areas, such as structural health and environmental monitoring. Vidal *et al.*, for example, demonstrated a 3D-printed encapsulated UHF sensor antenna in the 700 MHz to 1 GHz frequency range, where it was developed for early-stage and long-term concrete monitoring.<sup>155</sup> It was challenging to implant antennas and sensors inside concrete due to changes in permittivity and conductivity during the curing process, and over time, this caused strong attenuation and impedance mismatch for the embedded antennas. Concrete's dielectric properties tend to fluctuate rapidly, resulting in unreliable readings in early-stage monitoring. Moreover, to

maintain operational longevity, robust encapsulation was enforced so that one can withstand harsh conditions and uphold reliable transmission of signals. Therefore, a 3D-printed encapsulated biconical and miniaturized spiral antenna was fabricated using polyjet technology and photopolymer as the printing material. Significant advancements were demonstrated in mitigating impedance mismatch caused by concrete's permittivity shifts and loss tangent during curing; furthermore, durability against moisture, corrosion, and mechanical stress as well as the maintenance of the temperature stability was ascertained.

Another fundamental application is the large-area real-time monitoring of environment where it is crucial to be able to detect crisis situations (such as forest fires and industrial gas leakage) early on. In the work of Farooqui *et al.*, a low-cost fully integrated wireless sensor node was developed for the first time to monitor humidity, temperature, and hydrogen sulfide (H<sub>2</sub>S) gas.<sup>156</sup> Polyjet printing was utilized to fabricate the sensor package, capacitors, and circuit board using photocurable polymer as the main material. Inkjet printing was employed to deposit conductive and sensing materials directly onto the 3D-printed surfaces. The sensor antenna communicated in all directions since there was no mechanism to control its orientation in the environment. The 2.4 GHz dipole antenna was wrapped on a cube, such that most of the faces share a portion of the antenna. Zhang *et al.* proposed an inkjet-printed and cost-effective dipole antenna sensor for simultaneous strain and humidity sensing in structural health monitoring systems.<sup>107</sup> The sensor demonstrated sensitivities of  $\sim 24.03$  kHz per  $\mu\epsilon$  and  $\sim 12.38$  MHz per %RH, with minimal temperature influence between 25–45 °C. A backpropagation neural network was employed to decouple the strain and humidity responses, highlighting the antenna's multifunctionality despite challenges like low sensitivity in conventional designs.

Incorporating the machine learning algorithms into sensor antenna system designs can greatly have a positive effect on the capabilities of structural health and environmental monitoring. Large information generated by sensor antennas has been analyzed and interpreted in real time using machine learning so as to enable early identification of abnormalities that may cause environmental risks. For example, it is imperative to detect pipeline coating defects at an early stage in to avoid serious consequences. Defects in the coating of metal pipelines are often irregular and need accurate monitoring. Therefore, in this study by Zou *et al.*, an early detection system was proposed centered around machine learning processing and multi-resonator corrosion detection system using chipless RFID sensors.<sup>157</sup> The proposed RFID sensor system was composed of sensor array, microstrip transmitting/receiving antennas, and radar antennas. Another study for weather temperature prediction used various machine learning methods such as artificial neural networks (ANNs), random forests (RF), decision trees (DT), support vector machines (SVMs), and Gaussian processes (GPs). In this study, a half-mode substrate integrated waveguide (HMSIW) sensor antenna was used to categorize and project temperature ranges into three environmental settings:



early frost, normal, and early wildfire. The RF sensory intelligent system was able to enhance the performance, decrease energy consumption, and allow for autonomous real-time data recording.<sup>158</sup>

### 5.5 3D printing for antenna sensors for military and defense applications

A critical application of 3D-printed sensor antennas lies within the military and defense sector, where the interest is directed into four major sectors: sensors, computers and communications, projectiles, and other weapons and key technologies.<sup>159</sup> A comprehensive related technical review was presented by Bird *et al.* addressing the robustness of 3D printing technologies in the fabrication of advanced sensors tailored to military applications to offer protection from threats and to ensure real-time monitoring of physiological incidents.<sup>159</sup> In this review paper, the authors examined a number of 3D printing technologies in great detail, identified the need for the appropriate material compatibility, and laid strong emphasis to the resulting sensor properties.

## 6 Future outlook: challenges and open questions

In recent years, significant attention has been devoted to integrate 4D printing into sensor antenna systems, promising dynamic, self-adaptive systems with enhanced functionality and reduced geometrical complexity. This innovative approach has the potential to enable sensor antennas to respond intelligently to environmental changes, thereby leading to performance improvements and maximizing longevity. However, there are some hurdles that need to be overcome in the development of advanced smart materials, precise control over stimuli-driven transformations, long-term mechanical stability, and seamless integration with conventional electronics. In a comprehensive review, Carvalho *et al.* strongly emphasized on the difference in 3D printing material characterization and antenna parameters in contrast to 4D printing.<sup>160</sup> It was highlighted how characterization challenges were involved with applying stimuli that controls material properties over a factor of time. The authors presented various examples of the breakthrough in 4D printed antennas with the use of smart materials. Whether it is shape memory polymer (SMP)-based Ka-band heatsink antennas that unfold at certain temperatures, or bowtie antennas that adjust its bandwidth, or many other applications. Furthermore, the work of Sherburne *et al.* presented the fabrication of an S to X bands spiral antenna employing a controlled thermally responsive two-way shape memory alloy (SMA) that when stimulated transformed from a flat spiral antenna into a conical spiral antenna.<sup>161</sup> Selective laser melting (SLM) was the 3D printing technique employed for fabricating the nickel–titanium (NiTi) SMA. It is noted that the experimental validation was constructed to analyze changes due to different phase configurations. However, challenges arise due to material consistency and environment adaptability.

Another review study tackled a key topic concerning the use of metamaterials in 3D/4D printing of design and manufacturing of highly sophisticated, customizable structures for applications such as ultra-thin, lightweight, and broadband electromagnetic absorbers for stealth and electromagnetic interference (EMI) shielding, as well as novel antennas for next-generation wireless communications (5G/6G) and even adaptive or reconfigurable devices made from smart materials. Metamaterials have exceptional electromagnetic properties attributed to their engineered structures and not to their chemical composition. However, challenges may arise when the use of metamaterials is combined with 3D and 4D printing techniques. The challenges may include restrictions on printing material, surface roughness, accuracy during minuturization, mechanical endurance of certain composites, and manufacturing technique scalability. Furthermore, collaborative design of macro- and microstructures in order to maximize both electromagnetic and mechanical properties can be challenging, and current printing technologies usually fail to produce multi-material or multifunctional metamaterials in a single process. To fully exploit metamaterials' unique potential in practical applications, additional progress will be contingent on advances in printable material development, higher-resolution fabrication, and integrated design techniques.<sup>162</sup>

## 7 Conclusions

Antenna-based sensors represent a promising frontier in the design of compact, multifunctional, and energy-efficient sensing systems. By unifying the roles of wireless communication and environmental detection, these devices simplify system architecture while enabling real-time monitoring across diverse application domains. The inherent sensitivity of antenna structures to changes in their physical or dielectric environment, when coupled with smart material integration and advanced fabrication methods, opens the door to highly selective and adaptable sensing platforms. As demand grows for scalable, low-power, and distributed sensing in fields such as wearable health monitoring, infrastructure diagnostics, and the internet of things, antenna sensors are uniquely positioned to meet these challenges. Moving forward, continued interdisciplinary research into reconfigurable designs, material interfaces, and data-driven signal interpretation will be key to unlocking the full potential of antenna sensors as foundational elements for next-generation smart systems.

## Conflicts of interest

There are no conflicts to declare.

## Data availability

No primary research results, software or code have been included and no new data were generated or analysed as part of this mini review.



## References

- 1 H. Huang, *IEEE Sens. J.*, 2013, **13**, 3865–3872.
- 2 C. Reig and E. Avila-Navarro, *IEEE Sens. J.*, 2013, **14**, 2406–2418.
- 3 M. El Gharbi, R. Fernández-García, S. Ahyoud and I. Gil, *Materials*, 2020, **13**, 3781.
- 4 Y. Rahmat-Samii and E. Topsakal, *Antenna and sensor technologies in modern medical applications*, Wiley Online Library, 2021.
- 5 R. Bhattacharyya, C. Floerkemeier and S. Sarma, *Proc. IEEE*, 2010, **98**, 1593–1600.
- 6 T. Alam and M. Cheffena, *IEEE Trans. Microwave Theory Tech.*, 2022, **70**, 5289–5300.
- 7 J. Zhang, G. Y. Tian, A. M. Marindra, A. I. Sunny and A. B. Zhao, *Sensors*, 2017, **17**, 265.
- 8 A. Iqbal, A. Smida, O. A. Saraereh, Q. H. Alsafasfeh, N. K. Mallat and B. M. Lee, *Sensors*, 2019, **19**, 1200.
- 9 D. Prakash and N. Gupta, *Int. J. Microwave Wireless Technol.*, 2022, **14**, 19–33.
- 10 M. A. U. Haq, A. Armghan, K. Aliqab and M. Alsharari, *IEEE Access*, 2023, **11**, 40064–40074.
- 11 S. N. Mahmood, A. J. Ishak, T. Saeidi, H. Alsariera, S. Alani, A. Ismail and A. C. Soh, *Prog. Electromagn. Res. B*, 2020, **89**, 1–27.
- 12 P. V. Nikitin and K. S. Rao, *IEEE Antennas Propag. Mag.*, 2007, **48**, 212–218.
- 13 S. Zeadally, F. K. Shaikh, A. Talpur and Q. Z. Sheng, *Renewable Sustainable Energy Rev.*, 2020, **128**, 109901.
- 14 S. K. Koul and R. Bharadwaj, *Wearable antennas and body centric communication: present and future*, Springer Nature, 2021, vol. 787.
- 15 R. Raju, G. E. Bridges and S. Bhadra, *IEEE Antennas Propag. Mag.*, 2020, **62**, 76–89.
- 16 T. Le, Z. Lin, R. Vyas, V. Lakafosis, L. Yang, A. Traille, M. M. Tentzeris and C.-P. Wong, *J. Electron. Packag.*, 2013, **135**, 011007.
- 17 R. Singh, E. Singh and H. S. Nalwa, *RSC Adv.*, 2017, **7**, 48597–48630.
- 18 M. M. Tentzeris, A. Eid, T.-H. Lin, J. G. Hester, Y. Cui, A. Adeyeye, B. Tehrani and S. A. Nauroze, *Antenna and Sensor Technologies in Modern Medical Applications*, 2021, pp. 399–434.
- 19 S. Kim, *Electronics*, 2020, **9**, 1636.
- 20 C. Mariotti, W. Su, B. S. Cook, L. Roselli and M. M. Tentzeris, *IEEE Sens. J.*, 2014, **15**, 3156–3163.
- 21 N. Engheta and R. W. Ziolkowski, *Metamaterials: physics and engineering explorations*, John Wiley & Sons, 2006.
- 22 W. A. Awan, N. Hussain, S. G. Park and N. Kim, *Alexandria Eng. J.*, 2024, **92**, 50–62.
- 23 P. P. Kumar, K. Sreelakshmi, B. Sangeetha and S. Narayan, 2017 International Conference on Communication and Signal Processing (ICCSP), 2017, pp. 2081–2085.
- 24 R. Lin, H.-J. Kim, S. Achavananthadith, S. A. Kurt, S. C. Tan, H. Yao, B. C. Tee, J. K. Lee and J. S. Ho, *Nat. Commun.*, 2020, **11**, 444.
- 25 M. A. Farzin, S. M. Naghib and N. Rabiee, *ACS Biomater. Sci. Eng.*, 2024, **10**, 1262–1301.
- 26 J. Zhu and H. Cheng, *Sensors*, 2018, **18**, 4364.
- 27 D. H. Werner and S. Ganguly, *IEEE Antennas Propag. Mag.*, 2003, **45**, 38–57.
- 28 Y. I. Abdulkarim, L. Deng, H. Luo, S. Huang, M. Karaaslan, O. Altntas, M. Bakr, F. F. Muhammadsharif, H. N. Awl and C. Sabah, *et al.*, *J. Mater. Res. Technol.*, 2020, **9**, 10291–10304.
- 29 Y. Dong and T. Itoh, *Proc. IEEE*, 2012, **100**, 2271–2285.
- 30 C. Occhiuzzi, C. Paggi and G. Marrocco, *IEEE Trans. Antennas Propag.*, 2011, **59**, 4836–4840.
- 31 S. Kim and M. M. Tentzeris, *Int. J. Microwave Wireless Technol.*, 2018, **10**, 814–818.
- 32 M. Rizwan, A. A. Kutty, M. Kgwadi, T. D. Drysdale, L. Ukkonen and J. Virkki, 2016 10th European Conference on Antennas and Propagation (EuCAP), 2016, pp. 1–5.
- 33 S.-C. Lin and Y.-C. Liao, 2016 11th International Microsystems, Packaging, Assembly and Circuits Technology Conference (IMPACT), 2016, pp. 59–61.
- 34 H. Rahmani, D. Shetty, M. Wagih, Y. Ghasempour, V. Palazzi, N. B. Carvalho, R. Correia, A. Costanzo, D. Vital and F. Alimenti, *et al.*, *IEEE J. Microwaves*, 2023, **3**, 237–255.
- 35 A. R. Chishti, A. Aziz, M. A. Qureshi, M. N. Abbasi, D. Abbasi, S. S. Iqbal, A. Zerguine, A. M. Algarni and R. Hussain, *IEEE Access*, 2023, **11**, 104463–104484.
- 36 Z. U. Islam, A. Bermak and B. Wang, *Sensors*, 2024, **24**, 6355.
- 37 M. T. Khan, X. Q. Lin, C. Zhe and A. Saboor, *Front. Phys.*, 2024, **12**, 1402326.
- 38 M. Wagih and J. Shi, *IEEE Open J. Antennas Propag.*, 2022, **3**, 687–699.
- 39 W. Xia and Z. Zhang, *IET Nanodielectr.*, 2018, **1**, 17–31.
- 40 C. Luo, I. Gil and R. Fernandez-Garcia, *Meas. Sci. Technol.*, 2021, **32**, 105112.
- 41 M. A. Alsultan, S. López-Soriano and J. Melià-Segu, *IEEE Sens. J.*, 2025, **25**, 13974–13985.
- 42 P. B. A. Fechine, A. Tavora, L. C. Kretly, A. F. L. Almeida, M. R. P. Santos, F. N. A. Freire and A. S. B. Sombra, *J. Electron. Mater.*, 2006, **35**, 1848–1856.
- 43 F. M. Tchafa and H. Huang, *Smart Mater. Struct.*, 2018, **27**, 065019.
- 44 S. Di Meo, G. Matrone, M. Pasian, M. Bozzi, L. Perregrini, G. Magenes, A. Mazzanti, F. Svelto, P. Summers, G. Renne *et al.*, 2017 IEEE MTT-S International Microwave Workshop Series on Advanced Materials and Processes for RF and THz Applications (IMWS-AMP), 2017, pp. 1–3.
- 45 M. Z. Mahmud, M. T. Islam, N. Misran, A. F. Almutairi and M. Cho, *Sensors*, 2018, **18**, 2951.
- 46 I. Gagnadre, C. Gagnadre and J. Felon, *Electron. Lett.*, 1995, **31**, 1167–1168.
- 47 J. Siden, X. Zeng, T. Unander, A. Koptyug and H.-E. Nilsson, *SENSORS, 2007 IEEE*, 2007, pp. 308–311.
- 48 R. Bhattacharyya, C. Floerkemeier and S. Sarma, 2009 IEEE International Conference on RFID, 2009, pp. 95–102.



- 49 R. Bhattacharyya, C. Floerkemeier, S. Sarma and D. Deavours, 2011 IEEE International Conference on RFID, 2011, pp. 70–77.
- 50 M. Z. Mahmud, M. T. Islam, N. Misran, S. Kibria and M. Samsuzzaman, *IEEE Access*, 2018, **6**, 44763–44775.
- 51 M. A. Aldhaeabi, T. S. Almoneef, H. Attia and O. M. Ramahi, *IEEE Sens. J.*, 2019, **19**, 11867–11872.
- 52 H. R. Khaleel, H. M. Al-Rizzo, D. G. Rucker and S. Mohan, *IEEE Antennas Wireless Propag. Lett.*, 2012, **11**, 564–567.
- 53 N. A. Malik, P. Sant, T. Ajmal and M. Ur-Rehman, *IEEE J. Electromagn., RF Microwaves Med. Biol.*, 2020, **5**, 84–96.
- 54 W. Wang, X.-W. Xuan, W.-Y. Zhao and H.-K. Nie, *IEEE Sens. J.*, 2021, **21**, 14035–14042.
- 55 S. Vestrum, S. Abdollahi, M. Badv and Z. Abbasi, 2023 URSI International Symposium on Electromagnetic Theory (EMTS), 2023, pp. 25–27.
- 56 S. López-Soriano, P. Brunet, M. Alsultan and J. Meliá-Segu, *IEEE Sens. J.*, 2025, **25**, 7301–7309.
- 57 J. Meliá-Segu, R. Bhattacharyya, S. López-Soriano, X. Vilajosana and S. E. Sarma, *IEEE Sens. J.*, 2023, **25**, 27823–27833.
- 58 A. R. Eldamak and E. C. Fear, *Sensors*, 2018, **18**, 4088.
- 59 M. Baghelani, Z. Abbasi, M. Daneshmand and P. E. Light, *IEEE Sens. J.*, 2024, **24**, 9959–9969.
- 60 M. A. Ennasar, O. El Mrabet, K. Mohamed and M. Essaaidi, *Prog. Electromagn. Res. C*, 2019, **94**, 273–283.
- 61 H. M. Buttar, K. Pervez, M. M. U. Rahman, A. N. Mian, K. Riaz and Q. H. Abbasi, *IEEE Sens. J.*, 2023, **24**, 3574–3582.
- 62 S. I. Alekseev and M. C. Ziskin, *Bioelectromagnetics*, 2007, **28**, 331–339.
- 63 M. Benaissa, A. Chaabane, H. Attia and I. Al-Naib, *IEEE J. Microwaves*, 2025, **5**, 526–542.
- 64 H. Li, Y.-X. Guo, C. Liu, S. Xiao and L. Li, *IEEE Antennas Wireless Propag. Lett.*, 2015, **14**, 1176–1179.
- 65 M. Nosrati, A. Nosrati and F. Soltanian, *IEEE Sens. J.*, 2024, **24**, 40739–40748.
- 66 M. Zhang, Z. Liu, C. Shen, J. Wu and A. Zhao, *Materials*, 2022, **15**, 7851.
- 67 X. Li, S. Xue, L. Xie and G. Wan, *Struct. Health Monit.*, 2024, **23**, 3276–3295.
- 68 A. Daliri, A. Galehdar, W. S. Rowe, K. Ghorbani and S. John, *J. Intell. Mater. Syst. Struct.*, 2012, **23**, 169–182.
- 69 I. Mohammad and H. Huang, *Adv. Struct. Eng.*, 2011, **14**, 47–53.
- 70 S. Caizzone and E. DiGiampaolo, *IEEE Sens. J.*, 2015, **15**, 6767–6774.
- 71 M. Omer, G. Y. Tian, B. Gao and D. Su, *IEEE Sens. J.*, 2018, **18**, 9867–9873.
- 72 K. Bouzaffour, B. Lescop, P. Talbot, F. Gallée and S. Rioual, *IEEE Sens. J.*, 2021, **21**, 12306–12312.
- 73 H. Zhang, R. Yang, Y. He, G. Y. Tian, L. Xu and R. Wu, *Measurement*, 2016, **92**, 421–427.
- 74 I. El Masri, B. Lescop, P. Talbot, G. N. Vien, J. Becker, D. Thierry and S. Rioual, *Sens. Actuators, B*, 2020, **322**, 128602.
- 75 A. Z. Abbasi, N. Islam and Z. A. Shaikh, *et al.*, *Comput. Stand. Interfaces*, 2014, **36**, 263–270.
- 76 L. Ruiz-Garcia, L. Lunadei, P. Barreiro and J. I. Robla, *Sensors*, 2009, **9**, 4728–4750.
- 77 A. Raza, R. Keshavarz, E. Dutkiewicz and N. Shariati, *IEEE Trans. Instrum. Meas.*, 2023, **72**, 1–9.
- 78 J. Yao, F. M. Tchafa, A. Jain, S. Tjuatja and H. Huang, *IEEE Sens. J.*, 2016, **16**, 7053–7060.
- 79 M. Borgese, F. A. Dicandia, F. Costa, S. Genovesi and G. Manara, *IEEE Sens. J.*, 2017, **17**, 4699–4707.
- 80 L. Y. Liu, D. N. Lin, A. K. Poddar, U. L. Rohde and M. S. Tong, *IEEE Sens. J.*, 2024, **25**, 7107–7120.
- 81 N. T. Atanasov, B. N. Atanasov and G. L. Atanasova, *Electronics*, 2025, **14**, 544.
- 82 M. N. Rahman, S. A. Hassan, M. Samsuzzaman, M. S. J. Singh and M. T. Islam, *Microwave Opt. Technol. Lett.*, 2019, **61**, 361–364.
- 83 K. K. Kazemi, S. Hu, O. Niksan, K. K. Adhikari, N. R. Tanguy, S. Li, M. Arjmand and M. H. Zarifi, *Adv. Mater. Interfaces*, 2022, **9**, 2102411.
- 84 A. Bouchalkha and R. Karli, 2019 International Conference on Electrical and Computing Technologies and Applications (ICECTA), 2019, pp. 1–5.
- 85 P. K. Mishra, *Mater. Today: Proc.*, 2020, **29**, 561–567.
- 86 V. Patel, T. Chaware, P. Gundewar, A. Askhedkar, D. Pawar, A. Nagdeve and P. Gaikwad, ICCCE 2021: Proceedings of the 4th International Conference on Communications and Cyber Physical Engineering, 2022, pp. 689–700.
- 87 P. Soontornpipit, C. M. Furse, Y. C. Chung and B. M. Lin, *IEEE Trans. Antennas Propag.*, 2006, **54**, 797–800.
- 88 N. Haridas, A. El-Rayis, A. T. Erdogan and T. Arslan, Second NASA/ESA Conference on Adaptive Hardware and Systems (AHS 2007), 2007, pp. 14–19.
- 89 C.-H. Wu, T.-C. Huang and M. Ng Mou Kehn, *Sensors*, 2025, **25**, 3262.
- 90 M. Shaban, *Modelling*, 2025, **6**, 2.
- 91 S. Bhattacharya, A. K. Agarwal, O. Prakash, S. Singh, M. Pandey and R. Kant, *Sensors for automotive and aerospace applications*, 2019, pp. 1–6.
- 92 C. Waldschmidt, J. Hasch and W. Menzel, *IEEE J. Microwaves*, 2021, **1**, 135–148.
- 93 A. Nebylov, *Aerospace Sensors*, Momentum Press, 2012.
- 94 V. R. Kandregula, Z. D. Zaharis, Q. Z. Ahmed, F. A. Khan, T. H. Loh, J. Schreiber, A. J. R. Serres and P. I. Lazaridis, *Sensors*, 2024, **24**, 7395.
- 95 Z. Li, S. K. Sinha, G. M. Treich, Y. Wang, Q. Yang, A. A. Deshmukh, G. A. Sotzing and Y. Cao, *J. Mater. Chem. C*, 2020, **8**, 5662–5667.
- 96 L. Anchidin, A. Lavric, P.-M. Mutescu, A. I. Petrariu and V. Popa, *Sensors*, 2023, **23**, 1062.
- 97 R. Roges and P. K. Malik, *Int. J. Commun. Syst.*, 2021, **34**, e4940.
- 98 D. G. Arnaoutoglou, T. M. Empliouk, T. N. Kaifas, M. T. Chryssomallis and G. Kyriacou, *Electronics*, 2024, **13**, 3200.
- 99 A. Hamza, S. K. Prabhulingaiah, P. Pezeshkpour and B. E. Rapp, *Adv. Intell. Syst.*, 2025, **7**, 2400663.



- 100 T. Athauda and N. C. Karmakar, *Wireless Power Transfer*, 2019, **6**, 161–174.
- 101 S. Karuppuswami, S. Mondal, D. Kumar and P. Chahal, *IEEE Sens. J.*, 2020, **20**, 4679–4687.
- 102 W. C. Wilson and G. M. Atkinson, *IEEE Sens. J.*, 2014, **14**, 3745–3753.
- 103 K. S. Lay, L. Li and M. Okutsu, *HardwareX*, 2022, **12**, e00329.
- 104 M. Krchňák, J. Labun, J. Gamec, P. Kurdel and M. Českovič, 2018 XIII International Scientific Conference-New Trends in Aviation Development (NTAD), 2018, pp. 82–86.
- 105 K. N. Alvertos, E. A. Karagianni, K. D. Vardakis, T. K. Mpountas and D. I. Kaklamani, 2017 International workshop on antenna technology: Small antennas, innovative structures, and applications (iWAT), 2017, pp. 323–326.
- 106 R. A. S. I. Subad, L. B. Cross and K. Park, *Appl. Mech.*, 2021, **2**, 356–382.
- 107 J. Zhang, C. Li, Y. Gao, J. Tan, F. Xuan and X. Ling, *Sens. Actuators, A*, 2022, **347**, 113960.
- 108 R. C. Hansen, *Proc. IEEE*, 2005, **69**, 170–182.
- 109 A. Liu, Z. Huang, M. Li, Y. Wan, W. Li, T. X. Han, C. Liu, R. Du, D. K. Tan, J. Lu and Y. Shen, *IEEE Commun. Surv. Tutor.*, 2022, **24**, 994–1034.
- 110 M. Shahpari and D. V. Thiel, *IEEE Trans. Antennas Propag.*, 2018, **66**, 3894–3901.
- 111 Y. Liu, L. Xu, Y. Li and T. T. Ye, 2019 IEEE International Conference on RFID (RFID), 2019, pp. 1–6.
- 112 S. Khan, T. Mazhar, T. Shahzad, A. Bibi, W. Ahmad, M. A. Khan, M. M. Saeed and H. Hamam, *Discover Sustainability*, 2024, **5**, 412.
- 113 R. A. S. I. Subad, R. Ishraq, A. Dasgupta and S. Das, *ACS Appl. Mater. Interfaces*, 2025, **17**, 45056–45065.
- 114 W.-Y. Ko, L.-T. Huang and K.-J. Lin, *Sens. Actuators, A*, 2021, **317**, 112437.
- 115 Y. Zhu, J. Qin, G. Shi, C. Sun, M. Ingram, S. Qian, J. Lu, S. Zhang and Y. L. Zhong, *Carbon Energy*, 2022, **4**, 1242–1261.
- 116 A. Singh, B. Mandal, B. Biswas, S. Chatterjee, S. Banerjee, D. Mitra and R. Augustine, *IEEE Access*, 2024, **12**, 37179–37191.
- 117 A. Nicolle, S. Deng, M. Ihme, N. Kuzhagaliyeva, E. A. Ibrahim and A. Farooq, *J. Chem. Inf. Model.*, 2024, **64**, 597–620.
- 118 A. Sabbatella, A. Ponti, A. Candelieri and F. Archetti, *Mach. Learn. Knowl. Extr.*, 2024, **6**, 2232–2247.
- 119 D. Wang, J. Peng, Q. Yu, Y. Chen and H. Yu, *Sustainability*, 2019, **11**, 1919.
- 120 L. Yang, A. Zhu, J. Shao and T. Chi, *ISPRS Int. J. Geo-Inf.*, 2018, **7**, 63.
- 121 S. F. Pileggi, *Informatics*, 2025, p. 38.
- 122 A. K. Pandey and M. Singh, *J. Eng. Sci. Technol. Rev.*, 2024, **17**, 128–144.
- 123 A. Kalkal, S. Kumar, P. Kumar, R. Pradhan, M. Willander, G. Packirisamy, S. Kumar and B. D. Malhotra, *Addit. Manuf.*, 2021, **46**, 102088.
- 124 S. Abdollahi, E. J. Markvicka, C. Majidi and A. W. Feinberg, *Adv. Healthcare Mater.*, 2020, **9**, 1901735.
- 125 K. Tonyushkina and J. H. Nichols, *J. Diabetes Sci. Technol.*, 2009, **3**, 971–980.
- 126 H. Guan, T. Zhong, H. He, T. Zhao, L. Xing, Y. Zhang and X. Xue, *Nano Energy*, 2019, **59**, 754–761.
- 127 C. Zhao, Z. Xia, X. Wang, J. Nie, P. Huang and S. Zhao, *Mater. Des.*, 2020, **193**, 108788.
- 128 Z. Ma, S. Li, H. Wang, W. Cheng, Y. Li, L. Pan and Y. Shi, *J. Mater. Chem. B*, 2019, **7**, 173–197.
- 129 S. Nesaei, Y. Song, Y. Wang, X. Ruan, D. Du, A. Gozen and Y. Lin, *Anal. Chim. Acta*, 2018, **1043**, 142–149.
- 130 P. Salvo, R. Raedt, E. Carrette, D. Schaubroeck, J. Vanfleteren and L. Cardon, *Sens. Actuators, A*, 2012, **174**, 96–102.
- 131 R. Matta, D. Moreau and R. O'Connor, *Front. Neurosci.*, 2024, **18**, 1332827.
- 132 S. J. Kirubakaran, M. A. Bennet and N. Shanker, *Biomed. Signal Process. Control*, 2023, **85**, 105072.
- 133 W. Su, J. Zhu, H. Liao and M. M. Tentzeris, *IEEE Access*, 2020, **8**, 58575–58584.
- 134 S. Das, D. Mitra, A. S. Chezhan, B. Mandal and R. Augustine, *Front. Med. Technol.*, 2022, **4**, 924433.
- 135 A. Ahmed, U. Keshwala, V. Kumari and S. K. Dubey, *Measurement*, 2025, **250**, 117135.
- 136 P. Soontornpipit, *J. Med. Assoc. Thailand*, 2012, **95**, S189–S197.
- 137 U. Musa, A. Smida, M. S. Yahya, M. I. Waly, J. J. Tiang, N. K. Mallat, S. Muhammad and A. Salisu, *Sci. Rep.*, 2025, **15**, 30943.
- 138 A. Akohoule, D. Silue and O. Asseu, *et al.*, *J. Sens. Technol.*, 2024, **14**, 68–82.
- 139 T. Han, S. Kundu, A. Nag and Y. Xu, *Sensors*, 2019, **19**, 1706.
- 140 M. A. P. Mahmud, T. Tat, X. Xiao, P. Adhikary and J. Chen, *Exploration*, 2021, 20210033.
- 141 H. Yu, X. Zhang, H. Zheng, D. Li and Z. Pu, *Int. J. Bioprint.*, 2023, **9**, 722.
- 142 S. Koziel, A. Pietrenko-Dabrowska, M. Wojcikowski and B. Pankiewicz, *Sci. Rep.*, 2024, **14**, 26120.
- 143 M. Taştan, *Sensors*, 2025, **25**, 3183.
- 144 F. Angeletti, P. Iannelli, P. Gasbarri, M. Panella and A. Rosato, *Sensors*, 2022, **23**, 368.
- 145 A. Soumya, C. Krishna Mohan and L. R. Cenkeramaddi, *Sensors*, 2023, **23**, 8901.
- 146 O. A. Peverini, M. Lumia, G. Addamo, G. Virone and N. J. Fonseca, *IEEE J. Microwaves*, 2023, **3**, 800–814.
- 147 J. Teniente, J. C. Iriarte, R. Caballero, D. Valcázar, M. Goñi and A. Martínez, *IEEE Antennas Wireless Propag. Lett.*, 2018, **17**, 2070–2074.
- 148 G. Muntoni, G. Montisci, A. Melis, M. B. Lodi, N. Curreli, M. Simone, G. Tedeschi, A. Fanti, T. Pisanu and I. Kriegel, *et al.*, *IEEE Open J. Antennas Propag.*, 2022, **3**, 1351–1363.
- 149 V. Gjočaj, C. Crump, B. Wright and P. Chahal, 2020 IEEE 70th Electronic Components and Technology Conference (ECTC), 2020, pp. 666–670.
- 150 Z. Cai, Y. Zhou, Z. Weng, L. Deng, Y. Luo, M. Yu and Y. Qi, *IEEE Trans. Instrum. Meas.*, 2020, **69**, 8514–8525.



## Review

- 151 K. Lomakin, D. Simon, M. Sippel, K. Helmreich, E. Seler, Z. Tong, R. Reuter and G. Gold, 2018 48th European Microwave Conference (EuMC), 2018, pp. 1409–1412.
- 152 N. Mohan, F. Steinberger, S. Wächter, H. Erdogan and G. Elger, *Appl. Sci.*, 2025, **15**, 2676.
- 153 J. Fuchs, M. Gardill, M. Lübke, A. Dubey and F. Lurz, *IEEE Access*, 2022, **10**, 6775–6797.
- 154 C. Schüßler, M. Hoffmann, I. Ullmann, R. Ebel and M. Vossiek, *IEEE Access*, 2022, **10**, 40419–40431.
- 155 N. Vidal, J. Lopez-Villegas, I. Cairó, A. Garcia-Miquel, J. Romeu and L. Jofre, *Measurement*, 2025, **243**, 116439.
- 156 M. F. Farooqui, M. A. Karimi, K. N. Salama and A. Shamim, *Adv. Mater. Technol.*, 2017, **2**, 1700051.
- 157 Z. Y. Zou, W. Q. Li, Q. Y. Li, S. H. Jia and Y. J. Zhou, *IEEE Sens. J.*, 2024, **25**, 23460–23470.
- 158 A. T. Altakhaineh, R. Alrawashdeh and J. Zhou, *Energies*, 2024, **17**, 5208.
- 159 D. T. Bird and N. M. Ravindra, *Polymers*, 2021, **13**, 1455.
- 160 S. S. Carvalho, J. R. Reis and R. F. Caldeirinha, *IEEE Access*, 2024, **12**, 62861–62881.
- 161 M. Sherburne, K. Sibert, M. Daffron, A. Lennon, H. Feldmesser, J. Furer, K. Wolff, K. Pionke, P. Biermann and L. Bettwy, *et al.*, *ACS Appl. Eng. Mater.*, 2024, **3**, 44–50.
- 162 D. Yang, H. Mei, L. Yao, W. Yang, Y. Yao, L. Cheng, L. Zhang and K. G. Dassios, *J. Mater. Chem. C*, 2021, **9**, 12010–12036.

